LIMNOLOGY
and
OCEANOGRAPHY: METHODS

Limnol. Oceanogr.: Methods 10, 2012, 978–990

A multi-platform optical sensor for in situ sensing of water chemistry

Chee-Loon Ng[1], Schuyler Senft-Grupp[2], and Harold F. Hemond[2]*

[1]Center for Environmental Sensing and Modeling, Singapore-MIT Alliance for Research and Technology Centre, CREATE Tower Level 9, Singapore, 138602

[2]Department of Civil and Environmental Engineering, Building 48, Massachusetts Institute of Technology, Cambridge, MA, USA 02139

Abstract

A compact field-deployable optical instrument using fluorescence, absorbance, and scattering to identify and quantify contaminants and natural substances in water bodies is described. The instrument is capable of deployment on autonomous underwater and surface vehicles, manned vehicles, fixed platforms such as buoys, or access points in water supply or drainage networks. The instrument comprises (1) a flowcell, (2) multiple optical systems, (3) a data logger, (4) a power control board and computer, and (5) a battery. The instrument has been packaged in a cylindrical pressure case of 200 mm diameter and 300 mm length for electrically and mechanically seamless insertion as a STARFISH AUV payload module. The same module can be fitted with watertight end caps for use aboard other platforms, or simpler packaging can be employed for use in less demanding environments. For spectrofluorometry, the system uses six (expandable to twelve) electronically switchable excitation sources, allowing the construction of fluorescence excitation-emission matrices (EEMs). A deuterium-tungsten light source (185 to 1100 nm) is used in making UV-VIS absorbance measurements. Turbidity can be measured by nephelometry, using observations of light scattering at each excitation wavelength. The absorbance and turbidity capabilities provide useful water quality information and can also be used for correction of inner shielding effects. Validation of the instrument includes (1) comparison with a commercial luminescence spectrometer in measuring both standards and field samples, (2) comparisons of observed spectra with published optical characteristics for several chemicals, and (3) field demonstration aboard an AUV.

Understanding the chemistry of natural waters often relies on the collection of samples, followed by transport to a laboratory, and then by chemical analysis. This time-consuming and costly process introduces time delay and puts practical limits on the number of measurements that can be obtained in a given water body. Also, uncertainty can be introduced as samples undergo degradation during transport to the laboratory. Finally, low-density data sets obtained via manual sampling may fail to adequately capture spatiotemporal variability, which can sometimes hold the key to understanding biogeochemical processes in water bodies.

Recent developments in environmental in situ instrumentation and platforms have begun to address the above limitations. In the last decade particularly, there has been an increase in the use of in situ sensors and novel sensor platforms used as part of environmental sensing campaigns (Dickey 2009). Platforms include autonomous underwater vehicles (AUVs), autonomous surface vehicles (ASVs), buoys, and moorings (e.g., Smith et al. 2010; Vasilescu et al. 2010), and range widely in size, power availability, depth rating, mission duration, and communication capability. Chemical studies using AUV platforms have been carried out in oceans, and also more recently in lakes (e.g., Hemond et al. 2008; Caron et al. 2008). However, although AUV platforms are becoming

*Corresponding author: E-mail: kelvinng@smart.mit.edu

Acknowledgments

Funding for this work was provided by the Singapore National Research Foundation (NRF) through the Singapore-MIT Alliance for Research and Technology (SMART) Centre for Environmental Sensing and Modeling (CENSAM), MIT Sea Grant Project No. 2009-R/RCM-25, and the W. E. Leonhard professorship to Hemond. T. B. Koay, Y. H. Eng, Y. T. Tan, and J. L. Chew at the Acoustic Research Laboratory (ARL) of National University of Singapore (NUS) assisted with field deployment of the sensor on board their STARFISH AUV. We thank L. Gandois for sharing comparison data from lab-based instrument measurement, and M. Chitre and J. V. Sinfield for advice and helpful discussions. An international Patent Cooperation Treaty Application has been filed by Ng et al. 2012, based on the claims priority of US Provisional Application 61/477661, 61/494014, and 61/571593 by Ng et al. 2011.

DOI 10.4319/lom.2012.10.978

more available and easier to use, new and improved chemical sensor packages for these vehicles have been slower to materialize (Dickey 2009).

Chemical instrumentation suitable for autonomous in situ operation includes but is not necessarily limited to membrane-inlet mass spectrometers (Hemond et al. 2008), optical devices such as fluorometers and spectrophotometers, electrochemical sensors (e.g., Mueller and Hemond 2011), and flow injection analyzers. Each above type of sensor is intrinsically best suited to certain categories of substances (e.g., membrane-inlet mass spectrometry for gases but not humic materials, electrochemical sensors for ionic species but not most organic species). In the present case, we focus on optical sensing by means of fluorescence, absorbance, and scattering.

The potential to make optical measurements in situ has been enhanced by recent advances in light emitting diodes (LEDs), which are now available at reasonable cost in a wide range of wavelengths, from 245 nm through the infrared region (www.thorlabs.com). This enables LED-excited fluorescence spectrum measurements to be made at a substantial number of excitation wavelengths, thus providing two-dimensional data sets, often called excitation-emission matrices (EEMs). In this role LEDs offer several advantages over alternate narrowband light sources. Compared with broadband lamps paired with either monochromators or filters, LEDs generally have advantages of lower power usage, higher efficiency, cooler running temperatures, smaller size, and lower cost. Compared with laser sources, LEDs are less expensive and are available in a wider range of wavelengths. The negative aspects of LEDs typically include wider emission bands than those of lasers or sources using a lamp and monochromator; LEDs also often have lower power output and present more difficulty in focusing the beam as compared with laser sources (de Jong and Lucy 2006). Compared with EEMs obtained using excitation from a broadband lamp and monochromator, EEMs obtained using LED excitation typically contain a smaller number of excitation wavelengths, specific to the LEDs used. Nevertheless, the advantages of LEDs are compelling. LEDs have now been used in a wide range of optical-sensing devices (Oldham et al. 2000; Agbaria et al. 2002; Powe et al. 2004; Fletcher et al. 2006; Lowry et al. 2008; Powe et al. 2010), and researchers have begun to demonstrate field-capable instruments. For example, Obeidat et al. (2008) describe a 1.5 kg spectrofluorometer for analyzing plant and animal feed in the field, using excitation sources ranging from 405 to 640 nm; power is supplied by a laptop computer which also captures, stores, and analyzes the resulting EEMs. Other work includes the development of a single UV LED field spectrofluorometer for reagent-based characterization of selenium concentrations in river water (Suzuki et al. 2010) and a fiber optic in vivo LED fluorescence instrument for real-time medical imaging (Fabila et al. 2011).

Commercial suppliers such as WET Labs, Turner Designs, Seapoints, and YSI produce optical sensors specifically designed for measurements in natural waters, including spectrometers for absorbance measurements, turbidity sensors, and fluorometers for measuring specific compounds or chemical groups such as dissolved organic matter, crude oil, rhodamine, and chlorophyll. The sensors generally use a single LED excitation source and an emission detector with a filter, with LED and filter both chosen for the optimum wavelength bands for the parameter of interest. The output of a single-wavelength-pair fluorometer, however, is intrinsically incapable of identifying or correcting for interferences (Lambert et al. 2003). Ocean Optics and StellarNet both supply spectroscopy accessories such as spectrometers and fiber optics that are generally smaller, easier to use, and less expensive than typical laboratory equipment, and which have been applied to environmental analyses (Kuo et al. 2004; Fiorani and Palucci 2008; Obeidat et al. 2008; Suzuki et al. 2010; Fabila et al. 2011).

To the authors' knowledge, however, no low-cost instrument capable of deployment aboard a small AUV and exploiting both the spectral absorbance and the fluorescence EEM of natural waters yet exists. This article provides details for a field instrument, named LEDIF, that has been built to address this need, and is made possible by advances in LED technology, advances in commercially available optical components, advances in low-cost single board microcomputers, and a valuable growing literature discussing LED-based field instruments. LEDIF measures fluorescence, absorbance, and turbidity of natural waters. It is specifically designed for incorporation as a payload module of a STARFISH developed by National University of Singapore Acoustic Research Laboratory (Koay et al. 2011) or the MIT Sea Grant Reef Explorer, but with some variation in packaging can be used manually or can be installed on multiple other types of autonomous platforms. Applications include but are not limited to long-term monitoring, guiding rapid response to environmental chemical releases, developing adaptive sampling strategies for autonomous vehicles, and facilitating basic water quality research. This manuscript discusses the design and optical performance of LEDIF; equally important issues of signal processing will be discussed elsewhere.

Materials and procedure

Sensor module overview

The layout of LEDIF and its typical modes of deployment are shown in Fig. 1. The optical functions of LEDIF rely on a custom-designed flowcell fitted with light-emitting diodes (LEDs) of different wavelengths, focused on the analytical volume and oriented 90° from the main axis of light collection by a series of adjustable optics. To measure absorbance, a broadband (185 to 1100 nm) light source coupled via an optical fiber illuminates the flowcell at 180° to the light collection system. Turbidity is also measured within the flowcell using the nephelometry principle, at each LED wavelength. For all measurements (fluorescence, absorbance, and turbidity), light from the flowcell is observed with an Ocean Optics USB4000

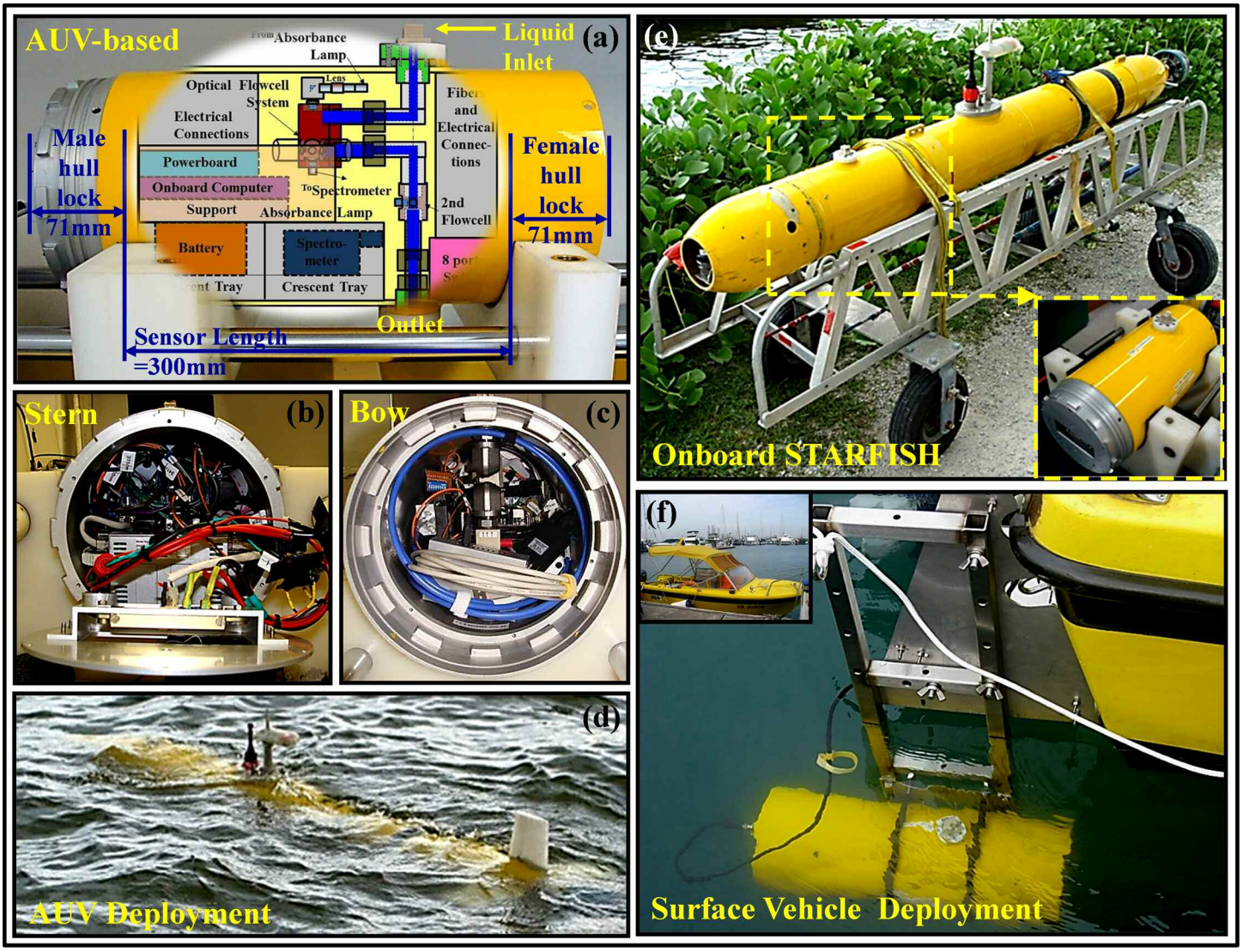

Fig. 1. The layout of LEDIF and the demonstration of its multi-platform deployment capability: (a, b, and c) Front, stern, and bow views of LEDIF packaged inside the pressure hull, (d) LEDIF aboard STARFISH deployed in the field for sensing of water chemistry, (e) LEDIF integrated to the STARFISH, and (f) LEDIF end capped for surface vehicles deployment, using a simple interface box for communication and external brackets.

spectrometer, and the data are recorded with a single board computer running custom software under a Linux operating system. LEDIF uses switching DC-DC converters to efficiently provide 5 and 12 volts DC (VDC) to various subsystems from either an internal battery or from any external power supply voltage between 12 and 72 VDC, a range that encompasses voltages used on a very large number of AUVs.

Flowcell geometry

A compact [~37(W) × 61(L) mm] optical flowcell permits the measurement of water's fluorescence spectrum, absorbance spectrum, and turbidity within the same analytical volume (Fig. 2). The optic junctions for optical attachment use UV transmissive fused silica windows with O-ring seals. Six junctions arranged perpendicular (90°) to the detecting optic junction are used to provide excitation to the analytical volume for fluorescence and turbidity measurements. A similar optic junction arranged directly opposite (180°) to the light-collecting optic junction is used to illuminate the volume for absorbance measurement. A collector lens, with focal length equal to the distance from the lens to the optical intersection with the perpendicular excitation optical paths, is fitted in front of the detecting optic junction to enhance collection of light emitted by fluorescence. Fluid flow into the flowcell occurs via a pathway that contains two 90° bends to minimize the entrance of stray light.

Excitation-emission optical system

A series of [~12.7(Dia) × 25.4(L) mm to 12.7(Dia) × 50.8(L) mm] LED-based light sources produce optical excitation for the analytical volume. The light produced by the LEDs is focused to the geometrical center of the flowcell, in line with

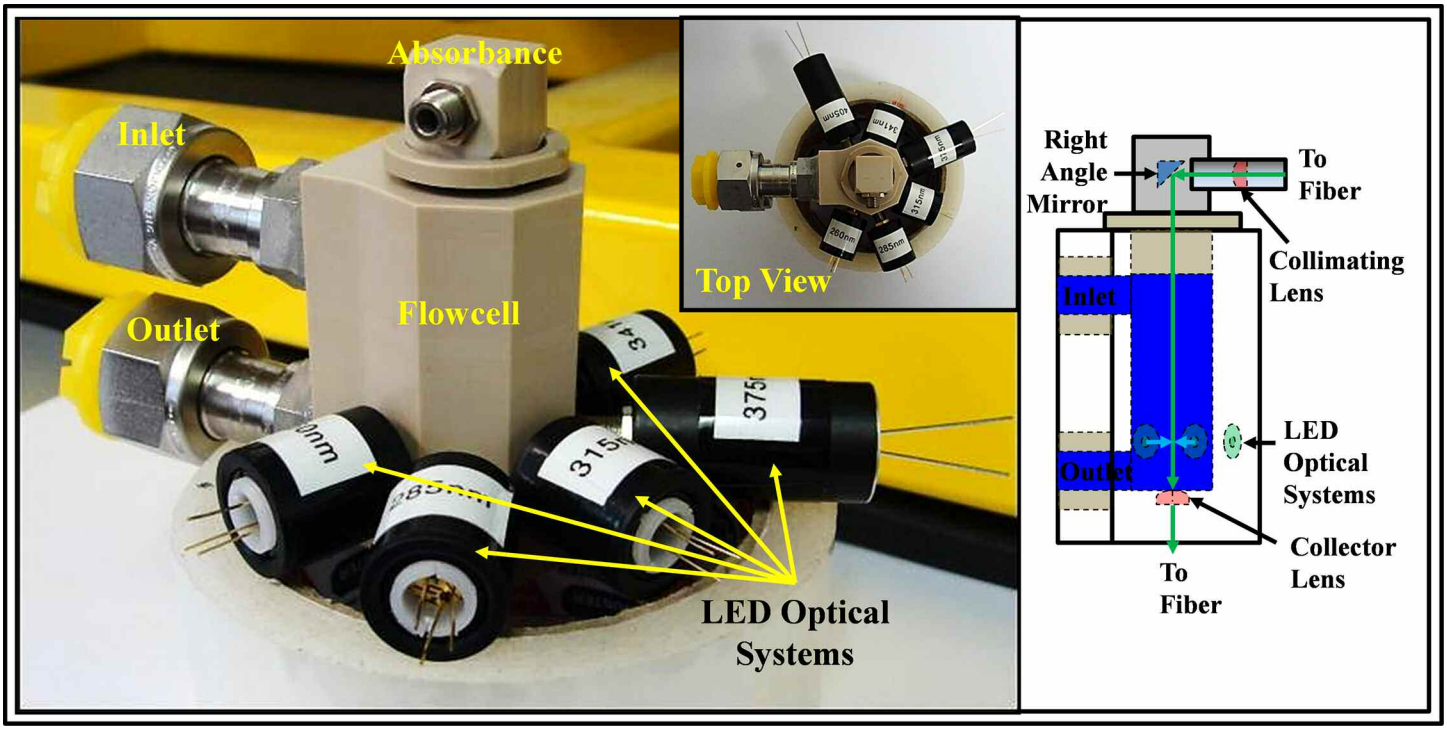

Fig. 2. LEDIF multi-excitation optical flowcell system.

the detection optical path, using compound lenses chosen to accommodate the divergence angle associated with each respective LED. The lenses are mounted inside lens tubes, and optical adjustments are performed using retaining rings, which are locked in place after adjustment to minimize susceptibility to mechanical disturbances. This compact packaging allows each excitation LED to be connected directly to the flowcell without the use of optical fiber, as shown in Fig. 2. For absorbance measurement, the light produced by a broadband (185 to 1100 nm) deuterium-tungsten (12 VDC at 0.6 A) source is focused with a plano-convex lens into an optical fiber, and the exiting light is collimated with another plano-convex lens and redirected with a right angle prism mirror to the optic junction of the flowcell. A collector lens with a single core fiber is used for the collection of photons from fluorescence and scattering, and for collection of transmitted light in absorbance mode.

Power control board

Fig. 3 shows the block diagram of the power control board of LEDIF, which powers various loads at 5 or 12 VDC. It provides efficient DC-DC conversion of external power at 12 to 72 VDC (e.g., from a 48 V AUV battery) to 5 VDC and 12 VDC. One 5 VDC output for the embedded computer is always on when the board is powered. Two outputs of 5 VDC at 2.5 A maximum and one output of 12 VDC at 2.5 A maximum are provided; these are used (at less than their maximum current ratings) to power the spectrometer and the deuterium-tungsten light source. Eight current-limited outputs at user selectable 5 VDC or 12 VDC, rated up to 100 mA, are provided for the excitation LEDs. Three 5 VDC software-controlled variable-current outputs are supplied for future expansion, such as alternate broadband light sources for absorbance measurement, or shorter-wavelength excitation sources that may become available in the future.

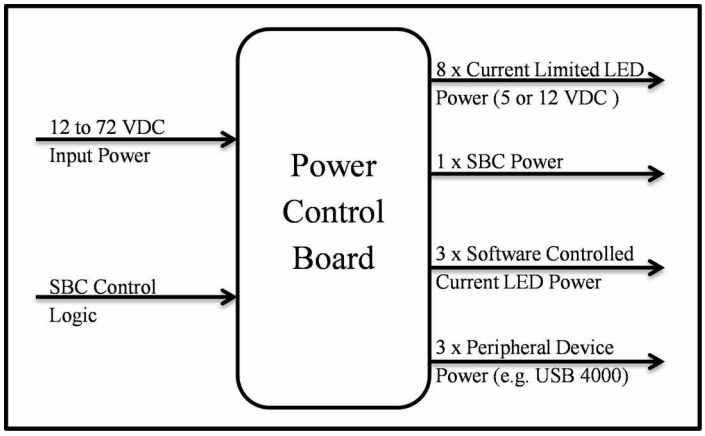

Fig. 3. Block diagram of LEDIF power control board.

Computer

The sensor is controlled by an onboard single-board-computer (SBC) manufactured by Technologic Systems (Model TS-7260-64-128F). The TS-7260 uses an ARM9 200 Mhz CPU with 64 MB of RAM, 128 MB of Flash memory, and 2 GB (expand-

able) USB flash storage, and runs a Debian Linux operating system (OS). The SBC has 3 serial COM ports, 2 USB ports, 1 Ethernet port, 30 digital input/output (DIO) pins, and two analog to digital converter (ADC) pins. The DIO and ADC pins are software controlled. A battery-backed real time clock retains synchronized sensor-host clock information for mission timestamps. An on-board temperature sensor allows direct measurement of board temperature in the field. The microcomputer uses Ethernet for communication with a host platform such as the STARFISH. In addition, a serial port (RS-232) can be connected to the SBC for software development and diagnostic purposes. The USB 2.0 (12 Mbits/s max) port is used for connection with the 2 GB of flash storage and a COM port is used for communication with the spectrometer (Ocean Optics USB4000). The microcomputer is connected to the power control board using the added TS-XDIO (PN: OP-XDIO) port. Further technical data can be found at http://www.embeddedarm.com/documentation/ts-7260-manual.pdf.

Software

Custom software (iLEDLIF; the extra "L" refers to the capability to control laser-excited instruments as well as LED-excited instruments) was written to control all sensor functionality. iLEDLIF was designed to be easily configurable and to handle asynchronous communication between multiple devices. The software is written in C++ using standard C/C++ libraries, and runs within Debian Linux on the embedded TS-7260 computer. iLEDLIF handles communication with external devices (e.g., spectrometer) over serial, USB, Ethernet, or DIO connections as well as with virtual devices implemented entirely in software (e.g., a data analysis device). On startup iLEDLIF reads an XML configuration file to load the device modules currently connected to the sensor, which allows for easy customization of the sensor hardware (e.g., changing excitation LEDs). Once all device modules have been initialized, iLEDLIF passes commands from the operator or AUV to the specific devices. iLEDLIF also has a built-in scripting language that enables users to generate text files of series of commands without needing to write or compile C++ code. These text files can be written or modified in the field, allowing the operator to automate scanning and spectra storing processes for a specific mission.

Spectrometer

Light transmitted through the sample volume or emitted by fluorescence from the sample volume is quantified by an Ocean Optics USB4000 spectrometer, which uses an uncooled TCD1304AP CCD (charge-coupled device) as its detector and is equipped with (1) UV4 Quartz windows, (2) variable long-pass order-sorting filters to block second- and third-order light (part number OFLV-4), (3) a cylindrical lens to increase light collection efficiency by the CCD (part number L4), and (4) the widest available entrance slit (200 × 1000 μm) to provide maximum light throughput. This slit width corresponds to a wavelength resolution of ~7.5 nm. Although the spectrometer is capable of higher resolution using narrower slit settings, this setting is acceptable given the characteristically broad fluorescence emission peaks of most analytes of interest, and the larger slit width allows for greater spectrometer throughput. The manufacturer-specified number of received photons per count of output is 130 and 60 at 400 nm and 600 nm, respectively. The optical bench uses an f/4 asymmetrical cross Czerny-Turner design with a SMA 905 inlet fitting, and has a 0.22 numerical aperture at the inlet that is matched to the connecting optical fiber. The integration time for each emission spectrum capture is software selectable from 3.8 ms to 10 s. Further technical information on the spectrometer is available at http://www.oceanoptics.com/technical/USB4000operatinginstructions.pdf.

Sample flow

To minimize power consumption when deployed on an AUV, LEDIF samples water without use of a pump, using ram pressure to drive fluid through the flowell as the AUV moves. To verify satisfactory flow conditions, three-dimensional transient flow modeling of the (x-z plane) symmetrical liquid chamber (meshed with 212,016 cells of hybrid hex/tet mesh) was performed with Fluent (Version 12) software. The typical (0.21 million cells) mesh captured flow features identical to those obtained with a high density (1.05 million cells) mesh [Fig. 4(d) and 4(e)], showing the adequacy of the chosen mesh density. Flow through a LEDIF mounted aboard a STARFISH was simulated for several vehicle velocities, to visualize the flow and determine if flow was obstructed, as well as to estimate the time required for water parcels both to reach the flowcell and to be flushed out. Each elbow was found to generate a local circulation that reduced the effective cross-sectional diameter of the flowpath. Particles were tracked to determine chemical transport and residence times; typical particle pathlines are shown in Fig. 4(b). The model shows that all tracked particles (335 particles tracked for high density mesh and 91 particles tracked for typical mesh) escape through the outlet, with the maximum transit time for 95% of particles plotted in Fig. 4(c) at various vehicle velocity conditions. Transit time was approximately 0.8 s at the standard 3 knot cruising speed of STARFISH.

Assessment

The performance of LEDIF was compared with that of a Perkin Elmer (PE) LS-55, a commercially available luminescence spectrometer that uses a pulsed xenon lamp (200 to 800 nm) as the source of excitation, and records emission spectra from 200 to 900 nm. The wavelengths in the PE LS-55 are selected with an excitation monochromator and an emission monochromator. The manufacturer's stated wavelength accuracy is ± 1 nm with a scanning speed of 10 to 1500 nm/min with 1 nm increments. The signal-to-noise ratio is stated as 2500:1 RMS at the baseline and 750:1 RMS for observing water Raman using 350 nm as excitation (http://www.perkinelmer.com/Catalog/Product/ID/L2250107).

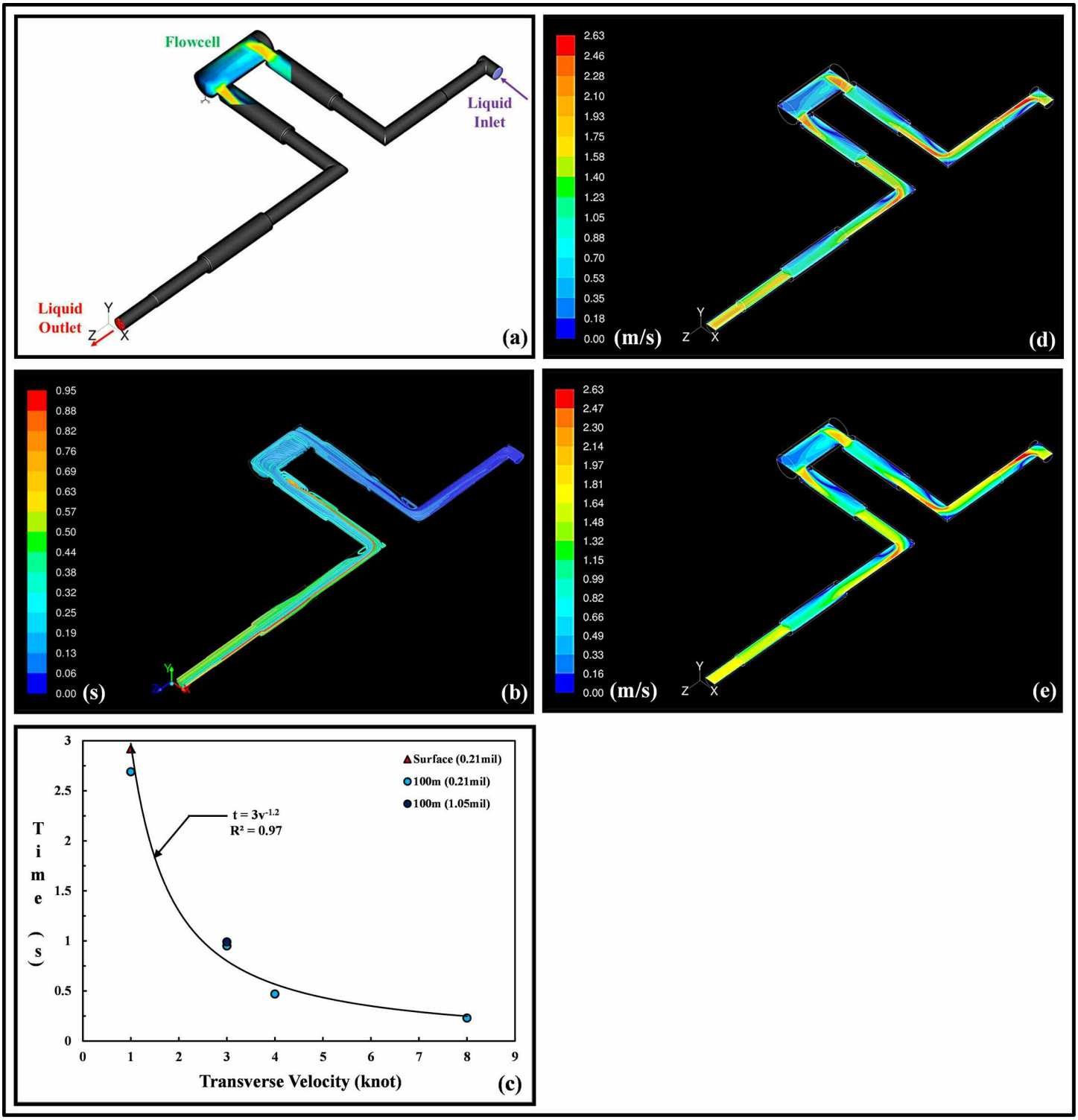

Fig. 4. 3-D transient modeling of through hull flow transportation manifold: (a) Liquid chamber of the through hull flow transportation manifold, (b) particle pathlines colored by elapsed time (s) at 100 m depth, 3 knots transverse velocity, (c) flow retention time at various operating conditions, and internal velocity contours (m/s) of (d) typical (0.21 million cells) and (e) high density (1.05 million cells) mesh at 100 m depth, 3 knots transverse velocity.

Fluorescence peak validation

Fluorescence peaks are assessed by comparing the fluorescence spectrum of an aqueous solution of rhodamine B and chlorophyll *a* (Chl *a*) measured with LEDIF against the corresponding spectrum from the PE LS-55 (Fig. 5). For spectrum display purposes, the emission spectrum intensity of the PE

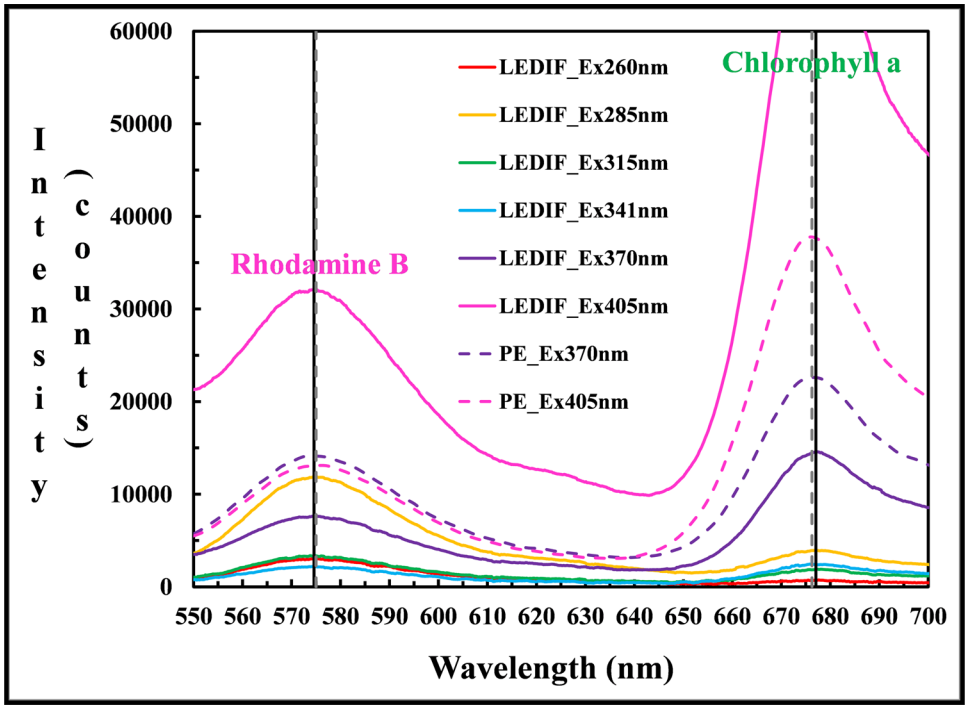

Fig. 5. Emission peaks comparison between LEDIF and Perkin Elmer LS-55 of a lab mixture (normalized by a factor equal to ~63.5). Note: Symbol legend in instrument_excitation wavelength format.

LS-55 is normalized by a factor equal to $I_{LEDIF(Saturation)}/I_{PE(Saturation)}$~63.5. The emission peaks of rhodamine B and Chl *a* observed by the two sensors are in excellent agreement, having percent differences in peak wavelength of 0.07% and 0.12%, respectively; the emission peaks of rhodamine B and Chl *a* reported by LEDIF were at 575 nm and 677 nm, respectively, agreeing well with values from the literature. For LEDIF, the peak amplitude of 405 nm is higher than 370 nm because the optical output of the 405 nm LED is approximately 4 times that of the 370 nm LED.

Field samples comparison

Emission spectra of pore waters collected from multiple depths at a peatland in Brunei are shown in Fig. 6. The fluorescence of these waters is attributed primarily due to high levels (10s of mg/L) of dissolved organic carbon (DOC). Emission spectra from LEDIF and the PE LS-55 are similar, and both LEDIF and the PE LS-55 instruments captured the small increase in the DOM concentration as the depth from which the samples were collected increased. A small shift of the fluorescence peaks between instruments may be due in part to slightly different excitation wavelengths, partly due to instrument design (differences in optical pathlengths), and partly due to degradation of the samples, which were stored for approximately 7 weeks between measurement with the two instruments; Shubina et al. (2010) have noted the heterogeneity of fluorophores in natural humic materials, which could lead to shifting of peaks as a result of differential rates of degradation (to the extent that this may be true, it underscores the potential value of in situ measurements). Cory et al. (2010) observed differences of up to 16 nm in peak locations of fulvic acid spectra as measured on three standard laboratory spectrofluorometers from different manufacturers.

Multi-spectral and EEM demonstration

The ability of LEDIF to capture an EEM is demonstrated by measuring an aqueous solution containing five chemicals, each relevant to natural water studies. 1 ppm naphthalene, 135 ppb pyrene, 5 ppm of a commercial humic acid, 0.2 ppm rhodamine B, and 5 ppm Chl *a* were selected to represent, respectively, a semi-volatile pollutant, a higher-molecular-weight PAH, humic material, a widely-used tracer, and algal bio-mass. Fig. 7 shows the EEM of the mixture: each chemical peak can be clearly identified by inspection. Wavelengths of individual emission peaks of the chemicals were compared with published fluorescence peaks from PhotochemCAD (Du et al. 1998) and found to be in very good agreement (Fig. 7). Note that many of the data in Du et al. (1998) are for compounds dissolved in a different solvent, potentially contributing to small differences in the location of fluorescence peaks.

Another meaningful comparison between LEDIF and the PE LS-55 is the instrumental detection limit (IDL), defined as: IDL = $C_{sample}/\{\text{average (I)}/[3\sigma(I)]\}$ where C_{sample} represents concentration of sample, I denotes intensity, and σ denotes standard deviation of multiple measurements at this concentration. Using an excitation wavelength of 405 nm for both instruments, the detection limit of rhodamine B was 2.5 ppb and 2.1 ppb for LEDIF and the PE LS-55, respectively. For an

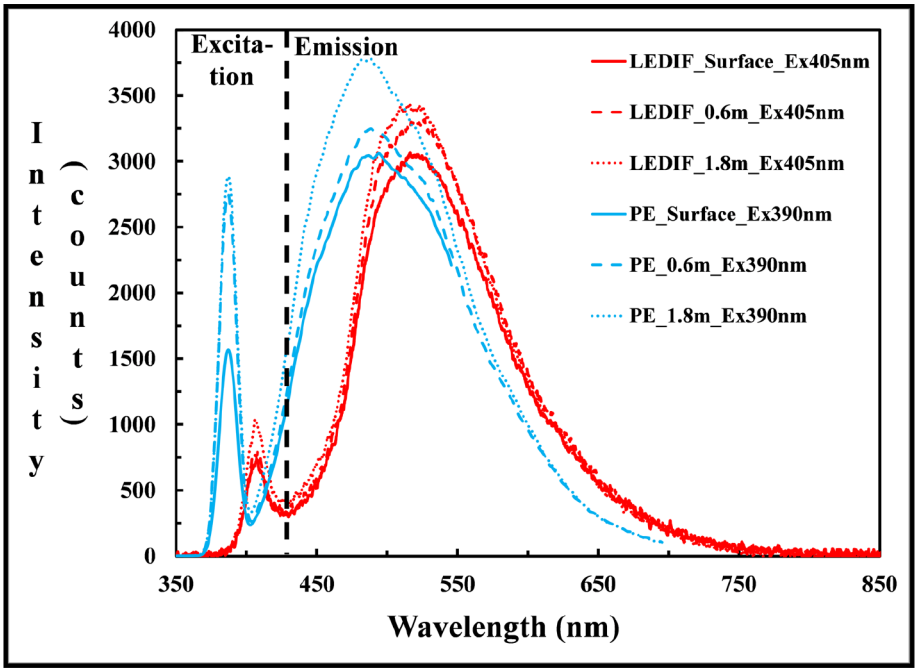

Fig. 6. Emission spectra from Brunei peatland water samples at various depths, observed using LEDIF and Perkin Elmer LS-55 (normalized by a factor equal to ~8). Aging of samples between measurements, differences in optical pathlengths, and small differences in excitation wavelength, likely contribute to the small wavelength shift in emission.

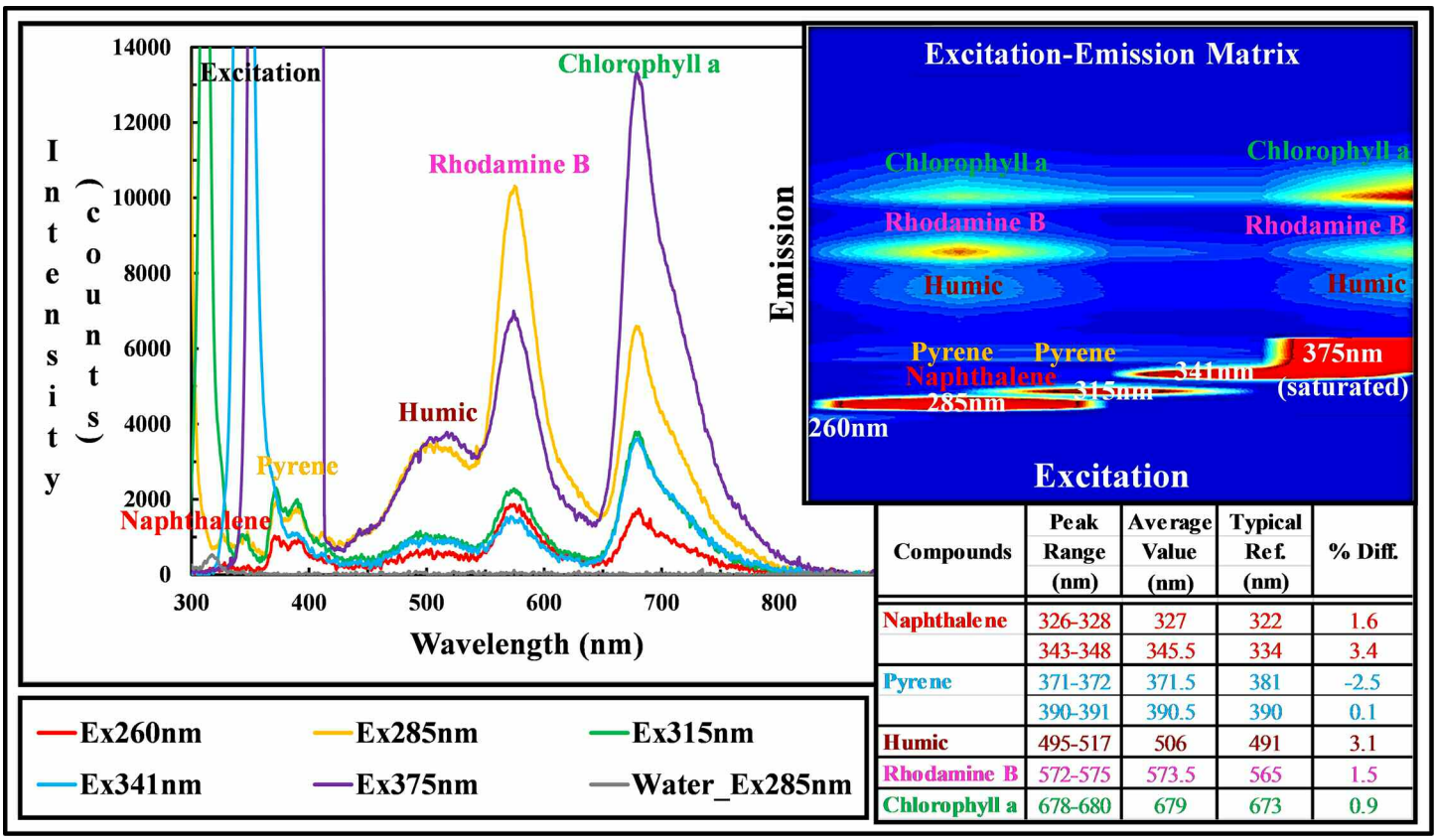

Compounds	Peak Range (nm)	Average Value (nm)	Typical Ref. (nm)	% Diff.
Naphthalene	326-328	327	322	1.6
	343-348	345.5	334	3.4
Pyrene	371-372	371.5	381	-2.5
	390-391	390.5	390	0.1
Humic	495-517	506	491	3.1
Rhodamine B	572-575	573.5	565	1.5
Chlorophyll a	678-680	679	673	0.9

Fig. 7. Emission spectrum and excitation-emission matrix of a complex lab mixture. Use of LEDs for excitation results in low cost and power consumption as well as rapid scanning when compared with a classical broadband light source used in conjunction with an emission monochromator.

excitation wavelength of 370 nm, the detection limit was 4 ppb and 3.2 ppb for LEDIF and the PE LS-55, respectively. For the mixture described above, LEDIF had a detection limit of ~50 ppb naphthalene, ~7 ppb pyrene, ~420 ppb humic acid, ~1 ppb rhodamine B, and ~5 ppb Chl *a*, with each detection limit being obtained at the optimum excitation wavelength.

Absorbance measurement

The absorption at various concentrations of aqueous rhodamine B at its wavelength of maximum absorbance is shown in Fig. 8(a). Based on Fig. 8(b), absorbance as low as 0.01 was adequately measured by LEDIF at this wavelength. The absorption peak is observed at 552 nm, which falls within the range of 550-554 nm (shaded region) reported by the manufacturer (Panreac). In addition, the profile of the absorbance curve recorded by LEDIF was compared with the graph published by PhotochemCAD using ethanol as solvent (Du et al. 1998) and found to be very similar. Based on linear fitting to the Beer-Lambert curve and the pathlength (4.0 cm) of LEDIF's flow-cell, the molar absorptivity was calculated as 0.17 cm^{-1} and the individual measurements at different concentrations are reported as 0.16 cm^{-1} (0.2 ppm), 0.19 cm^{-1}(1 ppm), and 0.17 cm^{-1} (2 ppm).

Turbidity measurement

Turbidity measurement was demonstrated using a calibration standard made of styrene divinyl benzene copolymer beads in water (AMCO CLEAR®TURBIDITY STANDARD manufactured by GFS Chemicals). Fig. 9 shows the scattered light spectra using 405 nm excitation and various levels of turbidity, as well as resulting calibration curves for turbidity in the 0 to 1 nephelometric turbidity unit (NTU) and 0 to 40 NTU ranges, using a 200 ms integration time. Three ranges of turbidity were tested: (1) 0 to 1 NTU in 0.2 NTU increments, (2) 0 to 10 NTU in 2 NTU increments, and (3) 0 to 40 NTU in 20 NTU increments. These ranges are representative of samples ranging from finished drinking water to many natural waters. 40 NTU does not reflect the upper bound limits of LEDIF, however, as higher turbidities can be measured by using shorter integration times, different excitation wavelengths, or lower optical power. Turbidity as low as 0.1 NTU can be measured, demonstrating a potential application in monitoring processed drinking water, for which a typical upper limit specified by water authorities is 1 NTU.

Pressure and temperature effects

Given that LEDIF is intended for in situ deployment, the sensor response as a function of pressure was assessed using Chl *a* as an example from 0 to 120 psi gauge pressure. It was found that the effect of pressure on sensor response was less than 2%. There is no evidence that LEDIF responds to temperature in any anomalous fashion. Fluorescence is known in general to decrease with increased temperature (Lakowicz 2006), although the dependence varies among compounds; Downing et al. (2012) have measured the temperature dependence for the case of DOM. The STARFISH vehicle, and likely most other platforms on which LEDIF would be deployed, carries a temperature sensor that may be used for temperature corrections if desired. A second possible temperature effect occurs via mechanisms that cause instrument response to vary with temperature. The USB4000 spectrometer CCD has 13 black pixels that are not exposed to incoming light, but are read each time that a spectrum is read from the instrument. The average of these pixels corrects for baseline offset for the resulting spectrum, whereas the variance among these pixels provides an estimate of the noise. These values are used in post processing to correct for temperature effects on the detector. We did not examine temperature effects that may exist due to various temperature coefficients of the LEDs, although users seeking the most precise data in environments of widely varying temperature, such as occur in a thermally stratified lake, might wish to measure appropriate correction factors. Typically, LED forward voltage decreases at rate of a

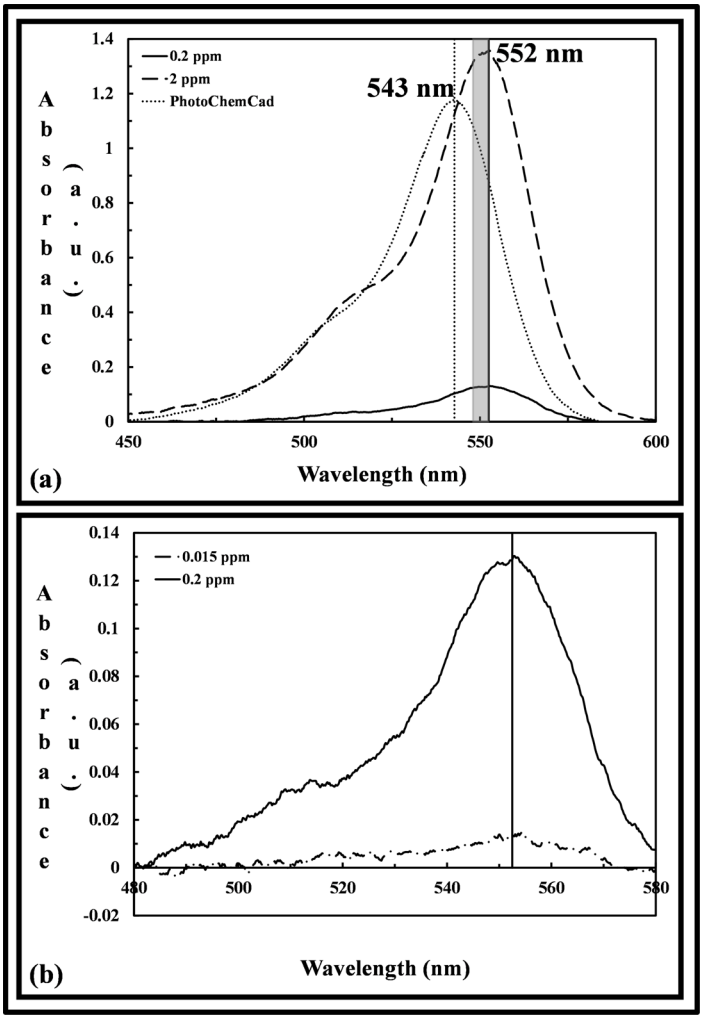

Fig. 8. (a) The absorption of rhodamine B dissolved in water as measured by LEDIF, compared with an absorbance spectrum reported by PhotoChemCAD for rhodamine B dissolved in ethanol, and (b) for low concentration samples, absorbance as low as 0.01 can be accurately measured.

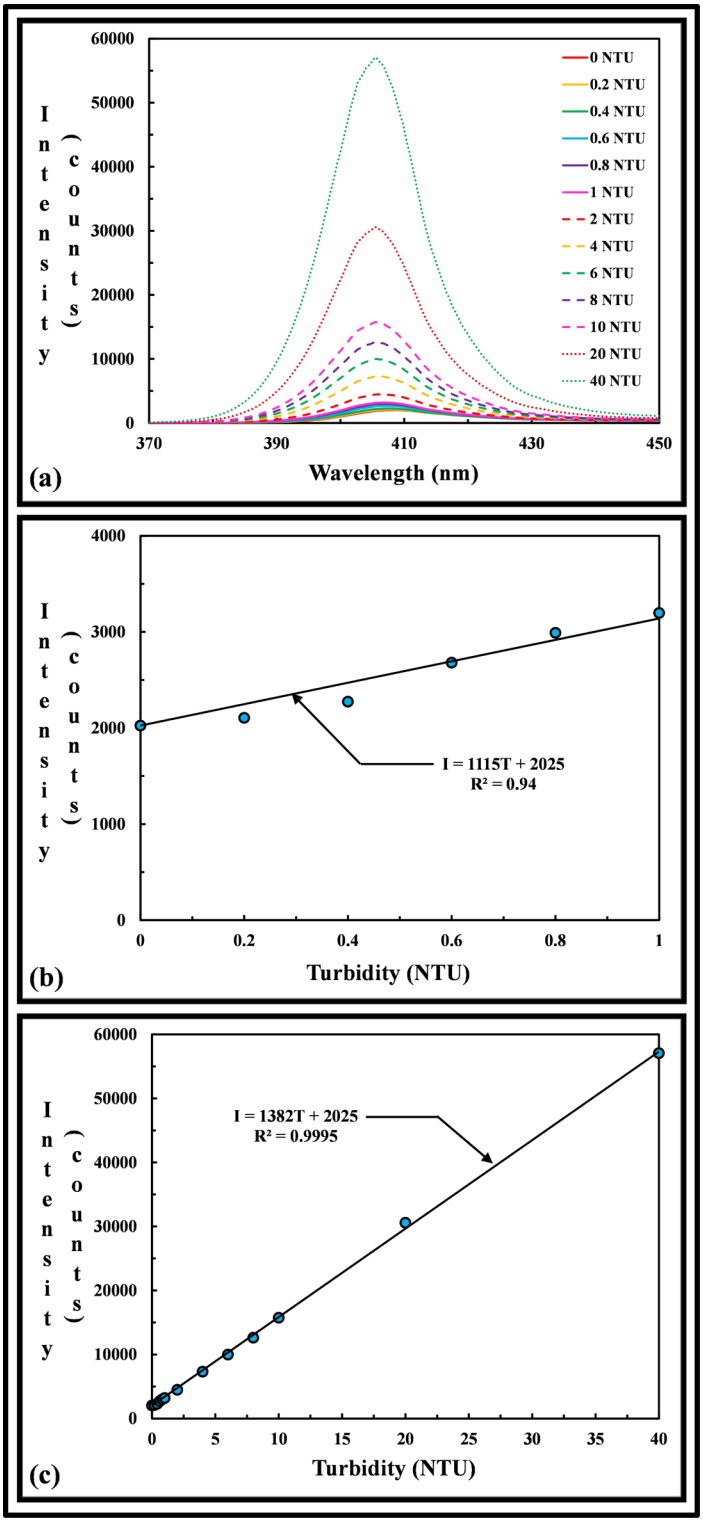

Fig. 9. Linear calibration curve for turbidity measurement of LEDIF: (a) Measurement of excitation light scattering of known turbidity standards, (b) turbidity below 1 NTU (typical requirement by water authorities) can be measured for the application of screening processed water, and (c) scattering of the excitation intensity can be calibrated and described with a single correlation for the turbidity (NTU) measurement.

few mV (out of several volts) per K.

Field deployment

Because an AUV host represents one of the more demanding platforms for in situ real time measurement, we present data demonstrating the successful operation of LEDIF as a payload for an AUV. Fig. 10 shows a 3-D subsurface mapping of Chl *a* concentration performed with LEDIF aboard STARFISH in the late morning of 20 Dec 2011 at Pandan reservoir, Singapore. In this demonstration, the vehicle covers an area of 150 × 80 m with an AUV "lawnmower" mission scheme, operating from the surface to 3 m depth (with 1 m increment) in one mission per depth. Total duration of the experiment, including all 4 missions was 1 h 26 min. The measurements demonstrated the successful operation of LEDIF in the freshwater environment for accessing the aforementioned information rapidly and with spatial resolution of 12 m.

Discussion

LEDIF is demonstrated to measure fluorescence excitation-emission matrices, optical absorbance, and light-scattering for a variety of substances of importance in natural waters. Turbidity as low as 0.1 NTU can be measured, and the instrument can operate autonomously aboard an AUV or surface vessel without requiring a sample pump. LEDIF can be built at moderate cost using mostly commercial off-the-shelf components; the materials bill for the unit tested here is approximately $15,000 Singapore dollars (order of $12,000 US dollars at the time of writing). Power consumption (0.5 W in standby mode, < 10 W in all active measurement modes) is low enough that it imposes only a minor energy burden on many typical AUV hosts; in fact, in deployments aboard STARFISH, LEDIF's internal battery was paralleled with the vehicle battery and actually subsidized the vehicle's energy budget. LEDIF software allowed the vehicle to manage operation of the instrument, a feature that is especially favorable where adaptive sampling, plume tracking, real-time monitoring as part of a network, or other advanced operating modes are envisioned. Table 1 shows the size, power consumption, and performance of LEDIF compared with three presently (at time of writing) available filter-type in situ commercial instruments.

Comments and recommendations

Because LEDIF relies on the transverse velocity of the host vehicle to create water flow through the flowcell, a pump may be needed to draw sample through the flowcell in the case of some alternate platforms (e.g., certain buoys). The flowcell was demonstrated to withstand > 10 bars of pressure without leakage; higher pressure versions are doubtless possible by using thicker quartz windows. If power consumption is of utmost importance and the absorption peak of the compound of interest falls within the wavelength range, the deuterium-tungsten lamp can be replaced by multi-wavelength LEDs. Optical design of a tri-wavelength package was investigated; it is expected that performance will be enhanced by improve-

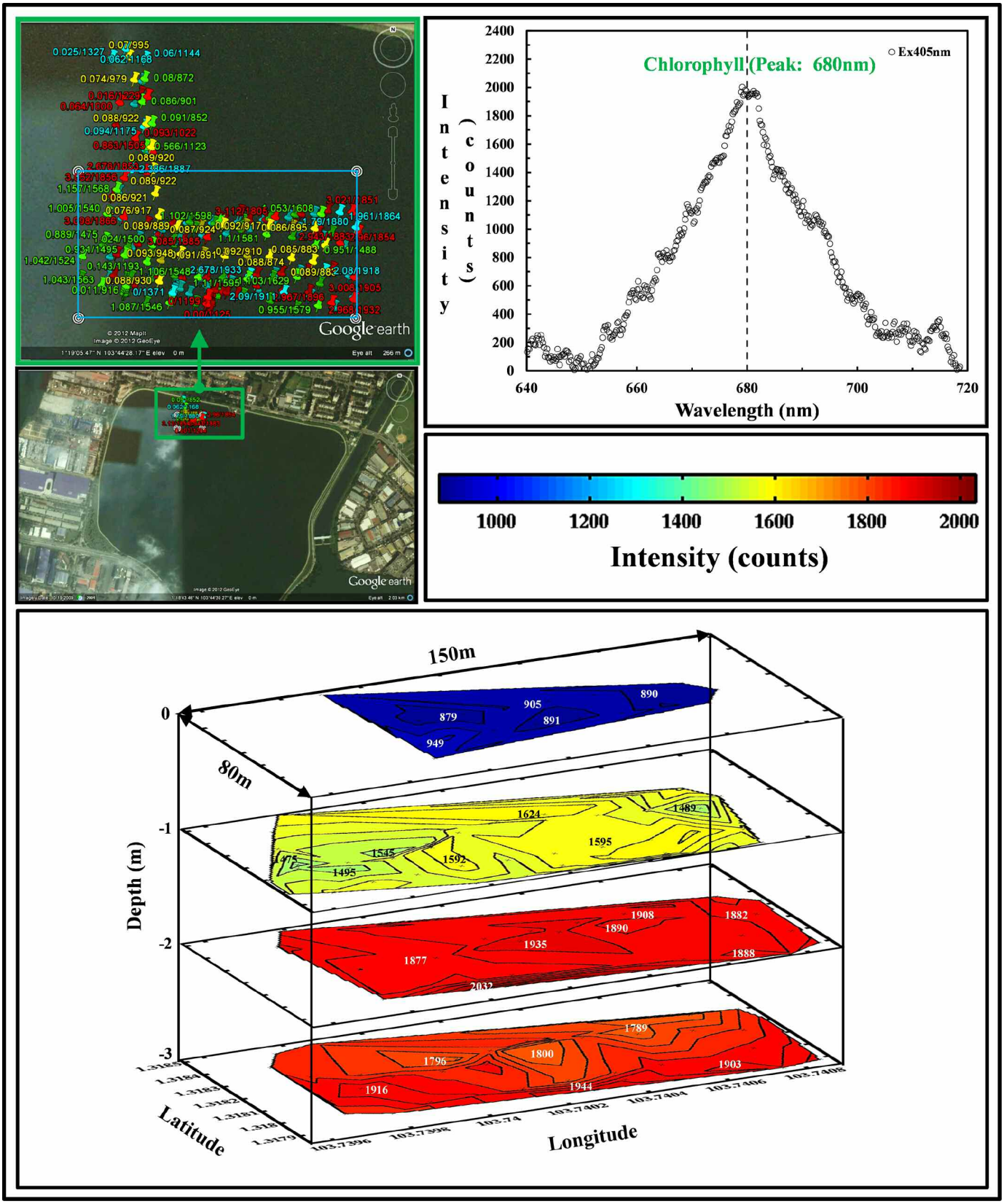

Fig. 10. 3-D subsurface mapping of Chl *a* concentration performed with LEDIF aboard STARFISH in the late morning of 20 Dec 2011 at Pandan reservoir, Singapore. The measurements demonstrated the successful operation of LEDIF in the freshwater environment for 3-D subsurface mapping.

Table 1. Comparison of LEDIF with filter-type in situ commercial instruments.

	LEDIF*		Wetlabs EcoFL†		YSI 600 OMS‡		Turner Designs C3™ Submersible Fluorometer§	
Size (volume, cm^3)	6000		396		750		1806	
Voltage (V)	12-7		27-15		External: 12		8-30	
Power (W), max.	2.6 (F‖, T¶), 9.5 (A#)		0.75		—		6	
Performance	**Range**	**Detection limit**	**Range**	**Resolution**	**Range**	**Resolution**	**Range**	**Resolution**
Chl *a* (µg/L)	0 to 1000	5	0 to 125	0.02	0 to 400	0.1	0 to 500	0.025
CDOM (µg/L)	0 to 150000	100	0 to 500	0.09	—	—	0 to 1250	0.15
Uranine (µg/L)	0 to 600	0.2	0 to 400	0.05	—	—	0 to 500	0.01
Rhodamine (µg/L)	0 to 1000	0.3	0 to 230	0.03	0 to 200	0.1	0 to 1000	0.01

*Standalone (sensor, power, and data logger) system with tri-optical measurement capability.
†ECO FL | WET Labs (http://www.wetlabs.com/eco-fl).
‡YSI 600OMS V2 Sonde-Single-Parameter, Low-Cost Water Quality Monitoring System (http://www.ysi.com/productsdetail.php?600OMS-5).
§Turner Designs C3™ Submersible Fluorometer. (http://www.turnerdesigns.com/products/submersible/c3-submersible).
‖F=Fluorescence.
¶T=Turbidity.
#A=Absorbance.

ments in commercially available LEDs, and will be reported in future work. At least two straightforward means are available for reducing the size and power consumption of LEDIF. For applications in which substantial on-board signal processing is not required, it is possible to replace the microcomputer with a microcontroller. We have demonstrated a version of LEDIF that uses an Atmel ATmega microcontroller and can be programmed using the popular Arduino programming language. The system consumes approximately 6 W during an active measurement (1 min or less) and less than 5 mW in sleep mode. It would also be possible to replace the USB4000 spectrometer with a subminiature spectrometer such as the Ocean Optics STS, whose volume is less than half that of the USB4000 and whose power consumption is only 0.75 watt (versus 1.25 watts for the USB4000). Low operational power consumption and an ultra-low power sleep mode make future versions of LEDIF well suited for remote installations where little power is available, such as remote installations using solar panels.

References

Agbaria, R. A., P. B. Oldham, M. McCarroll, L. B. McGown, and I. M. Warner. 2002. Molecular fluorescence, phosphorescence, and chemiluminescence spectrometry. Anal. Chem. 74:3952-3962 [doi:10.1021/ac020299z].

Caron, D. A., and others. 2008. Macro-to fine-scale spatial and temporal distributions and dynamics of phytoplankton and their environmental driving forces in a small montane lake in Southern California, USA. Limnol. Oceanogr. 53(5):2333-2349 [doi:10.4319/lo.2008.53.5_part_2.2333].

Cory, R, M., M. P. Miller, D. M. McKnight, J. J. Guerard, and P. L. Miller. 2010. Effect of instrument-specific response on the analysis of fulvic acid fluorescence spectra. Limnol. Oceanogr. Methods 8:67-68 [doi:10.4319/lom.2010.8.0067].

Dickey, T. 2009. Progress in multi-disciplinary sensing of the 4-dimensional ocean. Proc. SPIE. 7317:731702 [doi:10.1117/12.818068].

Downing, B. D., B. a. Pellerin, B. a. Bergamaschi, J. F. Saraceno, and T. E. C. Kraus. 2012. Seeing the light: the effects of particles, dissolved materials, and temperature on in situ measurements of DOM fluorescence in rivers and streams. Limnol. Oceanogr. Methods. 10:767-775 [doi:10.4319/lom.2012.10.767].

Du, H., R. A. Fuh, J. Li, A. Corkan, and J. S. Lindsey. 1998. PhotochemCAD: A computer-aided design and research tool in photochemistry. Photochem. Photobiol. 68:141-142.

Fabila, D. A., and others. (2011). Development of a spectrofluorometer with USB interface for in vivo measurements in surgical procedures, p. 1-4. *In* Circuit and Systems for Medical and Environmental Applications Workshop (CASME), 2010 2nd, 13-15 Dec 2010, Mexico City, Mexico. IEEE.

Fiorani L., and A. Palucci. 2008. Compact laser spectrofluorometer for water monitoring campaigns of southern italian regions affected by salinization and desertification processes. J. Optoelectr. Adv. Mat. 10(2):461-469.

Fletcher, K. A., and others. 2006. Molecular, fluorescence, phosphorescence, and chemiluminescence spectrometry. Anal. Chem. 78:4047-4068 [doi:10.1021/ac060683m].

Hemond, H. F., A. V. Mueller, and M. Hemond. 2008. Field testing of lake water chemistry with a portable and an AUV-based mass spectrometer. J. Amer. Soc. Mass Spectrom. 19(10):1403-1410 [doi:10.1016/j.jasms.2008.04.019].

de Jong, E. P., and C. A. Lucy. 2006. Low-picomolar of detection using high-power light-emitting diodes for fluorescence. Analyst 131(5):664-669 [doi:10.1039/b602193j].

Koay, T. B., and others. 2011. STARFISH—A small team of

autonomous robotic fish. Ind. J. Geo-Mar. Sci. 40:157-167.

Kuo, J. S., C. L. Kuyper, P. B. Allen, G. S. Fiorini, and D. T. Chiu. 2004. High-power blue/UV light-emitting diodes as excitation sources for sensitive detection. Electrophoresis 25(21-22):3796-3804 [doi:10.1002/elps.200406118].

Lakowicz, J. R. 2006. Principles of fluorescence spectroscopy, 3rd ed. Springer [doi:10.1007/978-0-387-46312-4].

Lambert, P., M. Goldthorp, B. Fieldhouse, Z. Wang, M. Fingas, L. Pearson, and E. Collazzi. 2003. Field fluorometers as dispersed oil-in-water monitors. J. Hazard. Mat. 102(1):57-79 [doi:10.1016/S0304-3894(03)00202-4].

Lowry, M., and others. 2008. Molecular fluorescence, phosphorescence, and chemiluminescence spectrometry. Anal. Chem. 80:4551-4574 [doi:10.1021/ac800749v].

Mueller, A. V., and H. F. Hemond. 2011. Towards an automated, standardized protocol for determination of equilibrium potential of ion-selective electrodes. Anal. Chim. Acta 690:71-78 [doi:10.1016/j.aca.2011.02.011].

Ng, C. L., H. F. Hemond, and S. Senft-Grupp. Date of filing: 20 Apr 2012. Highly compact multi-optical-junction optical flowcell and flexibly deployable optical sensing assemblies and systems for in-situ real-time spectroscopic measurements. International Patent Corporation Treaty Application. PCT/SG2012/000142.

Obeidat, S., B. Bai, G. D. Rayson, D. M. Anderson, A. D. Puscheck, S. Y. Landau, and T. Glasser. 2008. A multi-source portable light emitting diode spectrofluorometer. 62(3): 327-332.

Oldham, P. B., M. E. McCarroll, L. B. McGown, and I. M. Warner. 2000. Molecular fluorescence, phosphorescence, and chemiluminescence spectrometry. Anal. Chem. 72:197R-209R [doi:10.1021/a1000017p].

Powe, A. M., and others. 2004. Molecular fluorescence, phosphorescence, and chemiluminescence spectrometry. Anal. Chem. 76:4614-4634 [doi:10.1021/ac040095d].

———, and others. 2010. Molecular fluorescence, phosphorescence, and chemiluminescence Spectrometry. Anal. Chem. 82:4865-4894 [doi:10.1021/ac101131p].

Shubina, D., E. Fedoseeva, O. Gorshkova, S. Patsaeva, V. Terekhova, M. Timofeev, and V. Tuzhakov. 2010. The "blue shift" of emission maximum and the fluorescence quantum yield as quantitative spectral characteristics of dissolved humic substances. European Association of Remote Sensing Laboratories eProceedings 9:13-21.

Smith, R. N., and others. 2010. USC CINAPS Builds Bridges: observing and monitoring the Southern California Bight. IEEE Robot. Automat. Mag. 17(1):20-30 [doi:10.1109/MRA.2010.935795].

Suzuki, Y., N. Hashigaya, and S. Kawakubo. 2010. Development of a simple and low-cost device for fluorometric determination of selenium in water samples. Anal. Sci. Int. J. Jap. Soc. Anal. Chem. 26(6):719-722 [doi:10.2116/analsci.26.719].

Vasilescu, L., C. Detweiler, M. Doniec, D. Gurdan, S. Sosnowski, J. Stumpf, and D. Rus. 2010. AMOUR V: A hovering energy efficient underwater robot capable of dynamic payloads. Int. J. Robot. Res. 29(5):547-570 [doi:10.1177/0278364909358275].

Submitted 29 November 2011
Revised 8 November 2012
Accepted 16 November 2012